Review Article

Deep infiltrating endometriosis MR imaging with surgical correlation

Xue Tang[1], Rennan Ling[1], Jingshan Gong[1], Dongdong Mei[1], Yan Luo[1], Minge Li[2], Jianmin Xu[1], Liguo Ma[2]

[1]Department of Radiology, [2]Department of Gynaecology, Shenzhen People's Hospital, Second Clinical Medical College of Jinan University, Shenzhen 518020, China

Correspondence to: Dr. Jingshan Gong. Department of Radiology, Shenzhen People's Hospital, Second Clinical Medical College of Jinan University, Shenzhen 518020, China. Email: jshgong@sina.com.

Abstract: In this pictorial review, MR imaging findings of deep infiltrating endometriosis (DIE) are illustrated together with surgical correlation. DIE can appear as irregular nodules or plaques with similar signal intensity to muscle on both T1-weighted and T2-weighted images. Hemorrhage foci and strands or stellate margins are also often noted. Restriction of diffusion can be seen on diffusion-weighted image. Fibrosis and adhesions often result in morphologic changes, such as alimentary tract tortuosity, irregular or nodular thickening of uterosacral ligaments, and partial or complete obliteration of the pouch of Douglas. After intravenous gadolinium contrast agent administration, homo- or heterogeneous mild to moderate enhancement can be observed. MR imaging can depict endometriosis lesions and extension of DIE at different anatomic locations, which is well consistent with surgical findings. Combining signal and morphological abnormalities, MR imaging can diagnose and assess the extension of DIE with high accuracy. MR imaging findings of DIE facilitate surgeons at treatment decision making and patient communication.

Keywords: Deep infiltrating endometriosis; MR imaging; laparoscopic findings

Submitted Nov 30, 2017. Accepted for publication Jan 19, 2018.
doi: 10.21037/qims.2018.01.10
View this article at: http://dx.doi.org/10.21037/qims.2018.01.10

Introduction

Endometriosis, which is defined as the presence of ectopic endometrial tissue outside the uterus, is a common disease of premenopausal women with a prevalence of 5–20% and accounts for 20% of infertility and 24% of pelvic pain (1-5). Although ovaries are the most common sites for ectopic endometrial tissue implant, pelvic involvement and beyond, such as brain and lung, can be seen. Deep infiltrating endometriosis (DIE) is defined as subperitoneal invasion by endometriotic lesions that exceed 5 mm in depth (6). DIE is a common cause of pelvic pain, dysmenorrhea, dyspareunia, dyschezia, and urinary symptoms and is associated with infertility. Surgical treatment is required sometimes.

The diagnosis of DIE can be made through physical examination and laparoscopic exploration, followed by histologic confirmation. Disease extension assessment is difficult, especially in pelvic subperitoneal sites and in regions that are obscured by pelvic adhesions (7). Transvaginal ultrasonography (US) is usually the first imaging modality in diagnosis of endometriosis due to its accessibility and low cost. However, US is operator dependent and its poor penetration shows drawback in detecting endometriotic lesions in some location.

MR imaging is a noninvasive and nonionizing radiation imaging modality with high spatial resolution and excellent tissue identification through multi-parameter sequences. The broad field of view and multiplanar imaging allow MR imaging to survey the whole pelvis, which can facilitate the evaluation of lesion extension (8-10). In present pictorial review, we will exhibit DIE at different anatomic sites with surgical correlation.

MR imaging protocol

Patients with suspected DIE in our institution often

undergo pelvic MR imaging with following protocol: axial and sagittal high resolution turbo spin-echo T2-weighted sequences, transverse turbo spin-echo T1-weighted sequences with and without fat suppression, sagittal turbo spin-echo T1-weighted sequences with fat suppression, and transverse gradient-echo T1-weighted MR imaging with and without fat suppression before and after intravenous injection of gadolinium contrast agent with a dose of 0.2 mL per kilogram body weight. Coronal turbo spin-echo T2-weighted sequence and diffusion-weighted sequence are optional decided by radiologists.

MR features of endometriosis

Endometrial cyst

Ectopic endometriotic tissues generally implant in ovaries and result in endometriotic cysts (endometriomas) during repeated cyclic hemorrhage. The cysts typically contain thick, old dark blood called "chocolate cyst" (*Figure 1*). Therefore, unlike simple cysts which are low intensity on T1-weighted images and high intensity on T2-weighted images, endometriomas often shows both high intensity on T1-weighted images and T2-weighted images (*Figure 2*). Signal intensity of endometriomas can be low on T2-weighted image (*Figure 3*). A term called T2 shading sign defined as a cystic lesion with hyperintense signal on a T1-weighted image that demonstrates relative hypointensity on T2-weighted image (11). This phenomenon is secondary to the high concentration of protein and degraded blood products that result from the repeated hemorrhage, which shortens T2 relaxation due to susceptibility effect of degraded blood products. This sign was reported to have a specificity of 96% for endometriomas (12). Signal intensity characteristics of endometrial cysts sometimes mimic fat-containing lesions such as dermoids. Fat suppression sequences can distinguish mature cystic teratomas from endometrial cyst (*Figures 4,5*). Therefore, fat suppressed T1-weighted sequence is important in female pelvic imaging.

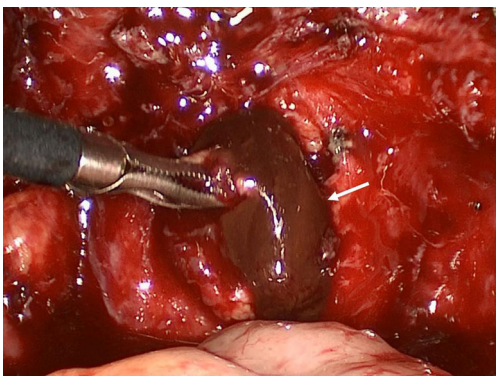

Figure 1 Laparoscopic photo shows chocolate-like dark old blood (arrow) spilling out after an endometriomas is cut open.

Deep infiltrating endometriosis

In DIE, the ectopic endometrial foci show secretary changes responding to circulating hormones and repeated bleeding (13). Hemorrhage causes inflammation, which induces histiocyte infiltration, fibromuscular hyperplasia and adhesion. The infiltration of histiocytes results in pigment

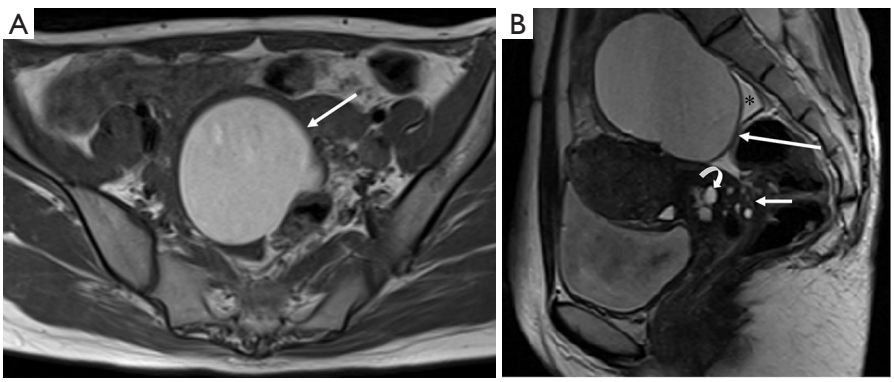

Figure 2 A 28-year-old woman with dyspareunia. (A) Transverse T1-weighted image shows a hyperintense lesion (arrow) in the site of right ovary; (B) sagittal T-weighted image shows the lesion is hyperintense (long arrow). A small amount of fluid in the pouch of Douglas (star), endometriotic lesion in posterior fornix (short arrow) and Nabothian cysts of cervix (curve arrow) are noted also.

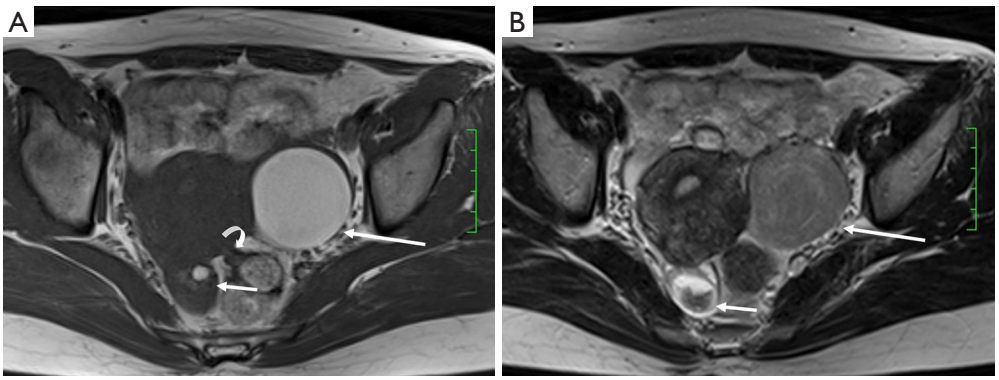

Figure 3 A 41-year-old woman with DIE. (A) Transverse T1-weighted image shows a homogeneous hyperintense cyst (long arrow) in the left ovary and a heterogeneous cyst (short arrow) with hyperintense component in the right ovary. Rectal wall involvement is seen (curve arrow); (B) transverse T2-weighted image shows hypointensity of both ovary lesions (long arrow and short arrow) consistent with T2 shading sign.

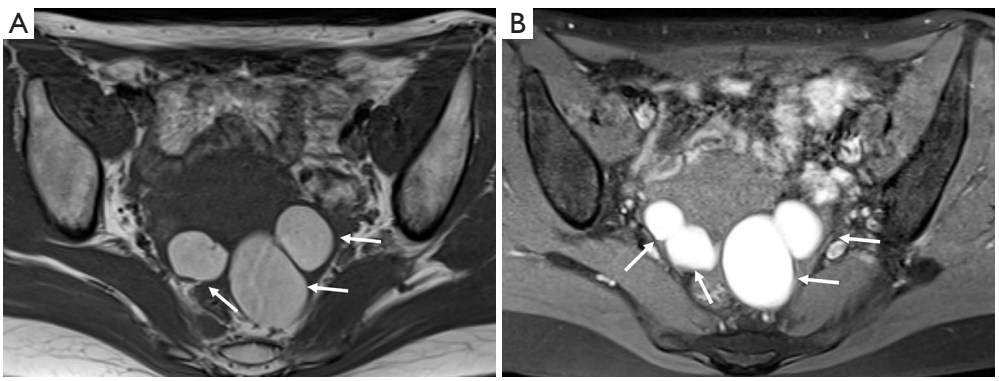

Figure 4 A 26-year-old woman with endometrioid cyst. (A) Transverse T1 weighted image shows several hyperintense lesions (arrows) in the pouch of Douglas; (B) fat suppression T1-weighted image demonstrates the signal of these lesions (arrows) is not suppressed.

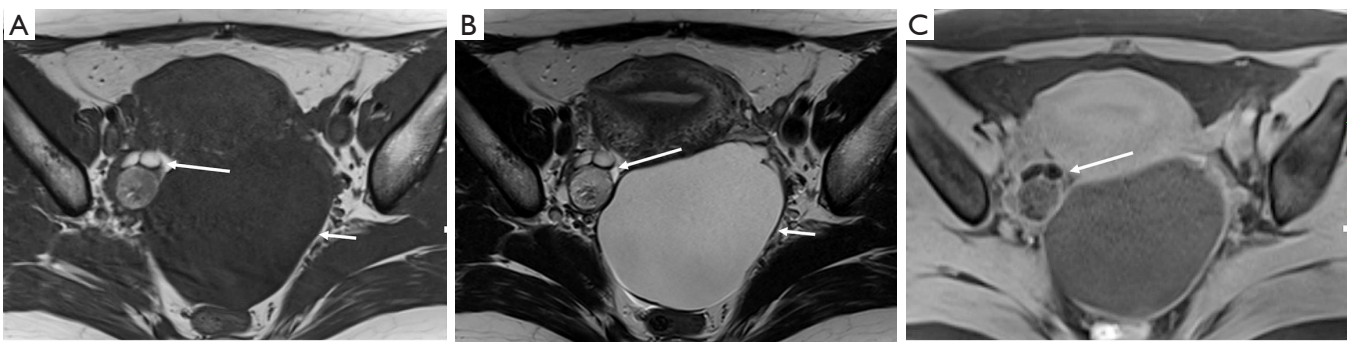

Figure 5 A 19-year-old girl with a mature teratoma at the right ovary and simple cyst at the left ovary. (A) Transverse T1-weighted image shows a lesion with hyperintensity (long arrow) at the site of right ovary and a low signal lesion (short arrow) at the pouch of Douglas; (B) transverse T2-weighted image shows the hyperintense lesion remains as hyper intensity (long arrow), while the hypointense lesion becomes high signal intensity (short arrow); (C) transverse fat suppression T1-weighted image demonstrates the hyperintense components on (A) are suppressed (arrow).

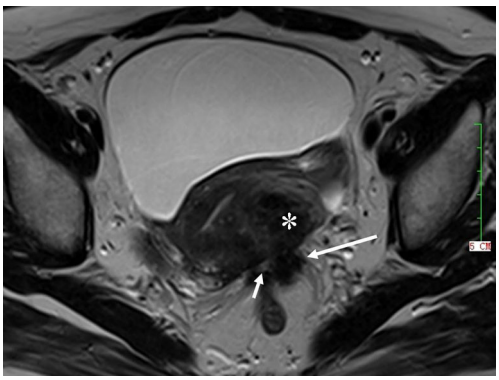

Figure 6 A 53-year-old woman with DIE. Transverse T2-weighted image shows an irregular hyperintense plaque (long arrow) with multiple hyperintense foci (short arrow) in the retrocervix. Adenomyosis (star) is demonstrated also.

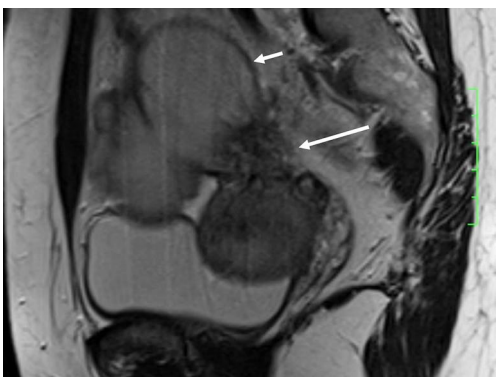

Figure 7 A 37-year-old woman with DIE. Sagittal T2-weighted image shows an irregular nodule (long arrow) with stellate margins in the right uterosacral ligament and an endometriotic cyst (short arrow).

laden with hemosiderin and hemofuscin, which accounts for hypointensity on T2 weight images, coupling with fibrosis. In some cases, endometriosis is stromal tissue dominated with little glands (14). Extensive adhesions can distort the normal pelvic anatomy and obliterate the pouch of Douglas.

DIE can affect all the pelvic structures in the following order: the rectovaginal septum and uterosacral ligaments (69.2% of cases), the vagina (14.5%), alimentary tract (9.9%), urinary tract (6.4%), and other extraperitoneal pelvic sites (15). At MR imaging, the diagnosis of DIE can be made by the joint presence of signal intensity abnormalities and morphologic abnormalities (8). The endometrial lesions often appear as irregular nodules or plaques with similar signal intensity to muscle on both T1-weighted and T2-weighted images, hemorrhage foci (*Figure 6*) and strands or stellate margins (*Figure 7*). Identifying hemorrhage foci is essential, especially on fat suppressed T1-weighted images (*Figure 8*). Restriction of diffusion can be seen within DIE on diffusion-weighted imaging, but on high b value imaging it often shows mild high intensity (*Figure 9*). After i.v. gadolinium, homo- or heterogeneous mild to moderate enhancement may be observed (*Figure 10*). Fibrosis and adhesions often result in morphologic changes, such as alimentary tract tortuosity, irregular or nodular thickening of uterosacral ligaments, and partial or complete obliteration of the pouch of Douglas (*Figures 11,12*). The morphologic abnormalities, demonstrated by MR imaging, show well consistence with laparoscopic findings (*Figures 12,13*). Another advantage of MR imaging is that it can depict endometrial lesions at different anatomic sites at single imaging, so that it can evaluate the extension of DIE

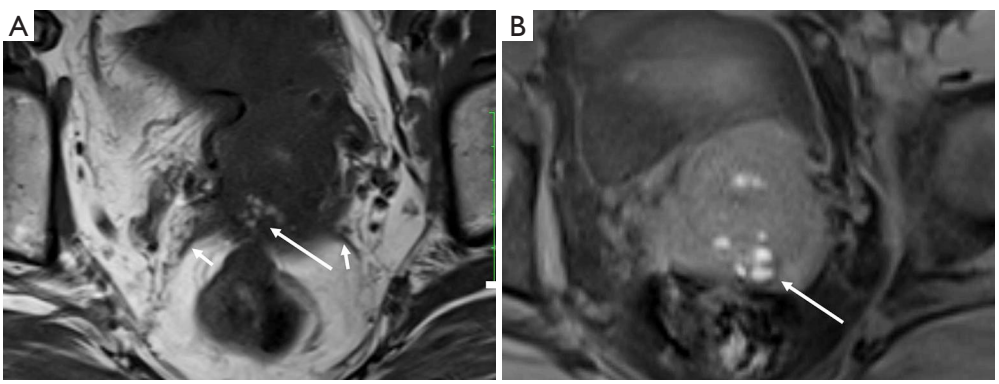

Figure 8 A 37-year-old woman with DIE. (A) Transverse T1-weighted image shows irregular hypointense plaque (long arrow) with multiple hyperintense foci at retrocervix. Thickening of bilateral uterosacral ligaments (short arrows) is noted; (B) transverse fat suppressed T1-weighted image shows signal of the hyperintense foci (arrow) on (A) remains unchanged and is more obvious.

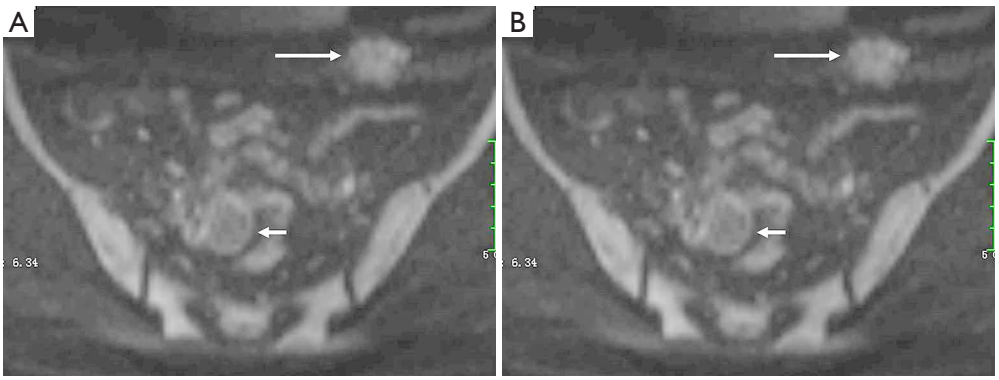

Figure 9 A 28-year-woman with DIE. (A) Transverse diffusion-weighted image with a b value of 500 s/mm^2 shows a hyperintense lesion (long arrow) in the left-low abdominal wall and an endometrial cyst (short arrow) in the right ovary. (B) Transverse diffusion-weighted image with a b value of 1,000 s/mm^2 shows the intensity of the abdominal wall lesion (long arrow) decreased and the right ovarian cyst (short arrow) as low signal intensity.

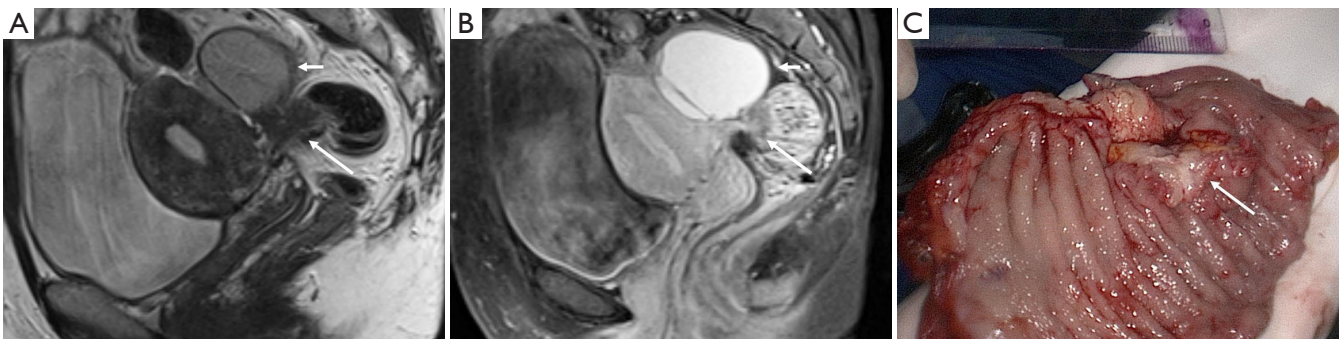

Figure 10 A 40-year-old woman with DIE. (A) Sagittal T2-weighted image depicts an irregular fibromuscular plaque (long arrow) involving anterior rectal wall, and an endometrial cyst (short arrow). (B) Sagittal contrast-enhanced fat-suppressed T1-weighted image shows mild heterogeneous enhancement of rectal wall lesion (long arrow). The endometrial cyst (short arrow) is noted. (C) Photograph of gross specimen demonstrates the endometrial lesion (arrow) penetrating the mucous layer of rectal wall.

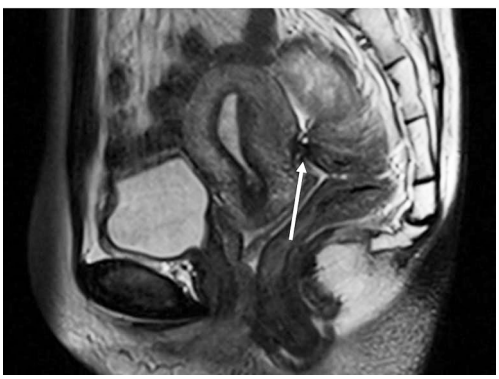

Figure 11 A 28-year-old woman with DIE. Sagittal T2-weighted image shows retrocervical endometriosis (arrow) and adhesion which results in distortion of rectum.

with high accuracy (8), especially degree of alimentary tract involvement (*Figure 14*) and ureter (*Figure 15*), which can guide treatment decision.

Malignant transformation of endometriosis

Although malignant transformation of endometriosis is rare complication with an occurrence rate of 0.6–0.8% (16-18), the possibility should be kept in mind when a radiologist is confronted with DIE. Contrast-enhanced mural nodules within an endometrial cyst often suggest malignant transformation (19). Hyperintensity due to hemorrhage makes it difficult to identify the enhancement. Dynamic subtraction MR imaging is useful in depicting small

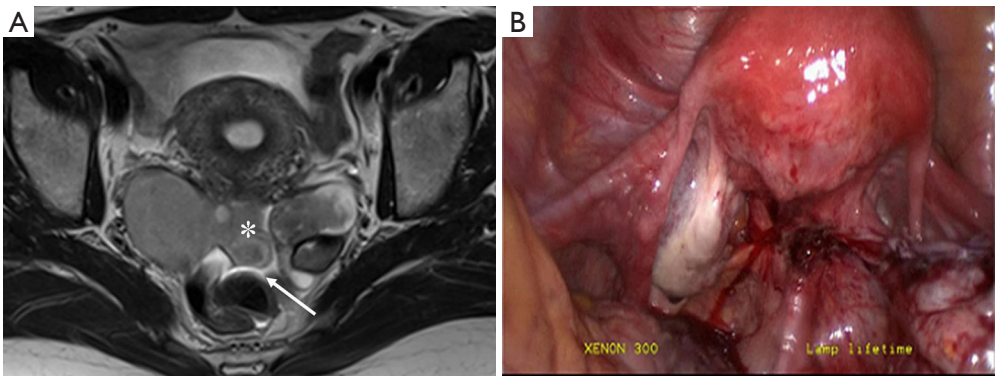

Figure 12 A 38-year-old woman with DIE. (A) Transverse T2-weighted image shows endometrial cysts (star) obliterating the pouch of Douglas and unsymmetrical fluid (arrow); (B) laparoscopic photo demonstrates obliteration of the pouch of Douglas. The endometrial cysts have been removed.

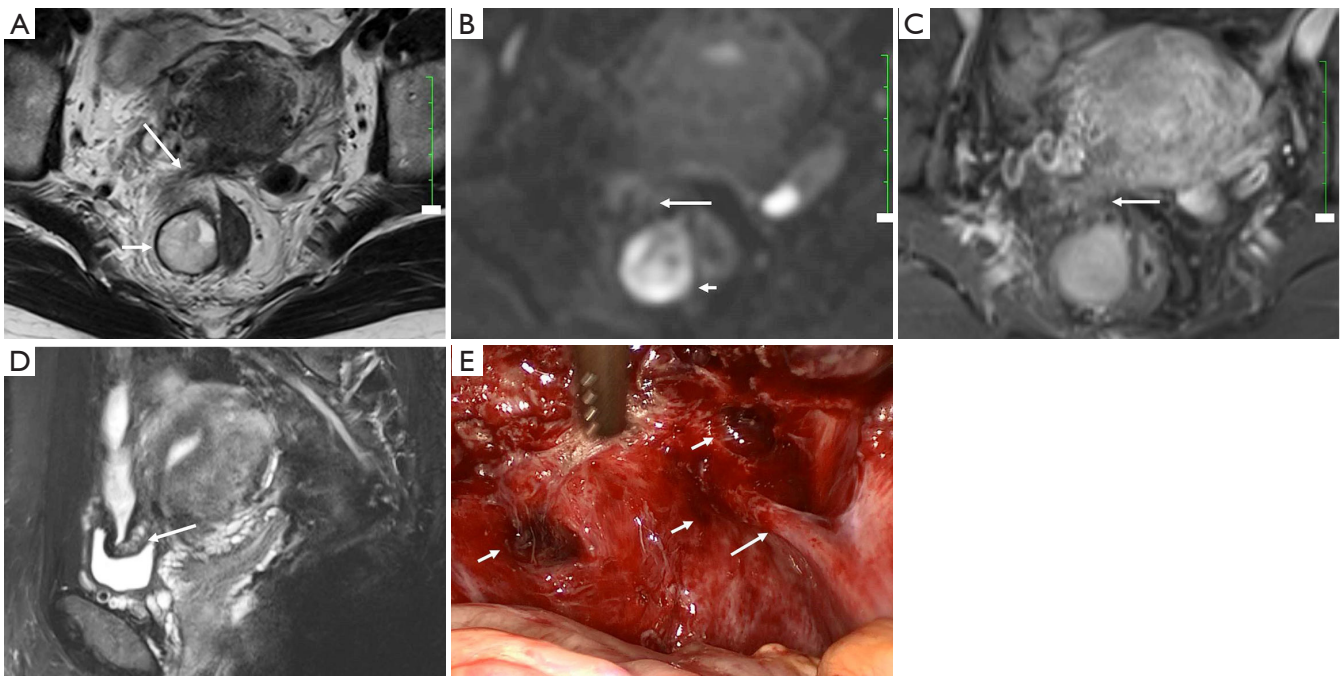

Figure 13 A 42-year-woman with DIE. (A) Transverse T2-weighted image shows thickening of the right uterosacral ligament (long arrow) and an endometrial cyst (short arrow) in the right perirectal fossa. (B) Transverse diffusion-weighted image with a b value of 1,000 s/mm^2 shows slight high signal of the right uterosacral ligament (arrow). The endometrial cyst (short arrow) in the right perirectal fossa is heterogeneously hyperintense, which may result from T2-through effect. (C) Transverse fat-suppressed T1-weighted image after iv gadolinium shows mild enhancement of the left uterosacral ligament (arrow). The endometrial cyst (short arrow) in the right perirectal fossa is noted also. (D) Sagittal fat suppressed T2-weighted image shows infiltration of the upper external aspect of the bladder wall (short arrow). (E) Laparoscopic photo shows thickening of the right uterosacral ligament (long arrow) and several subperitoneal endometrial lesions (short arrows).

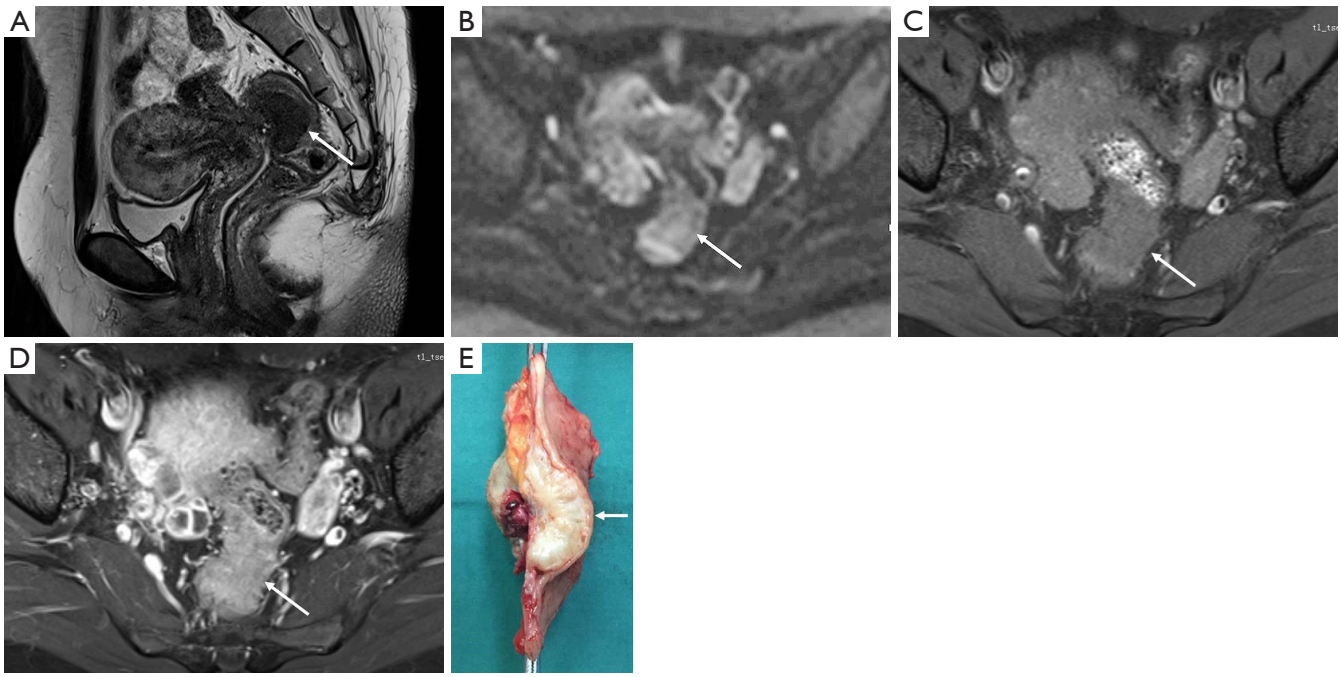

Figure 14 A 37-year-old woman with DIE. (A) Sagittal T2-weighted image shows a fan-shaped hypointense mass (arrow) infiltrating the wall of rectosigmoid; (B) transverse diffusion-weighted image shows the mass (arrow) is iso-intense to the bowel wall; (C) transverse fat-suppressed T1-weighted image shows the mass (arrow) is iso-intense to the muscle; (D) transverse contrast-enhanced fat-suppressed T1-weighted image shows the mass (arrow) demonstrates moderate homogenous enhancement; (E) photograph of gross specimen shows a fan-shaped lesion infiltrating the bowel wall with an intact mucosal surface (arrow).

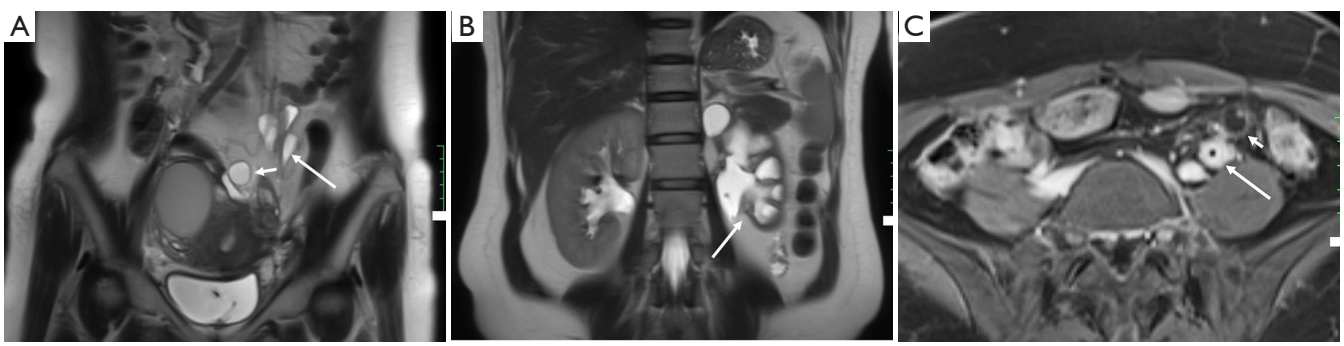

Figure 15 A 42-year-old woman with DIE. (A) Coronal pelvic T2-weighted image shows several endometrial cysts (long arrow) surrounding the left ureter. Endometrial cysts (short arrow) are depicted in the pouch of Douglas; (B) coronal abdominal T2-weighted image depicts hydronephrosis of left kidney (arrow); (C) contrast enhance transverse T1-weighted image demonstrates enhancement of the thickening left ureter (long arrow) and an endometrial cyst with wall enhancement (short arrow).

contrast-enhanced nodule within hyperintense endometrial lesions. Enlargement or disappearance of T2 shading of an endometrial lesion during follow-up suggests malignant transformation also. Diffusion-weighted imaging may also be helpful in differentiating DIE from carcinoma (20). Carcinoma often shows high signal intensity on high b value diffusion-weighted images, while DIE appears to be moderate signal on high b value diffusion-weighted images (*Figure 16*).

In summary, MR imaging can detect lesions of DIE at different anatomic structure through visualizing signal

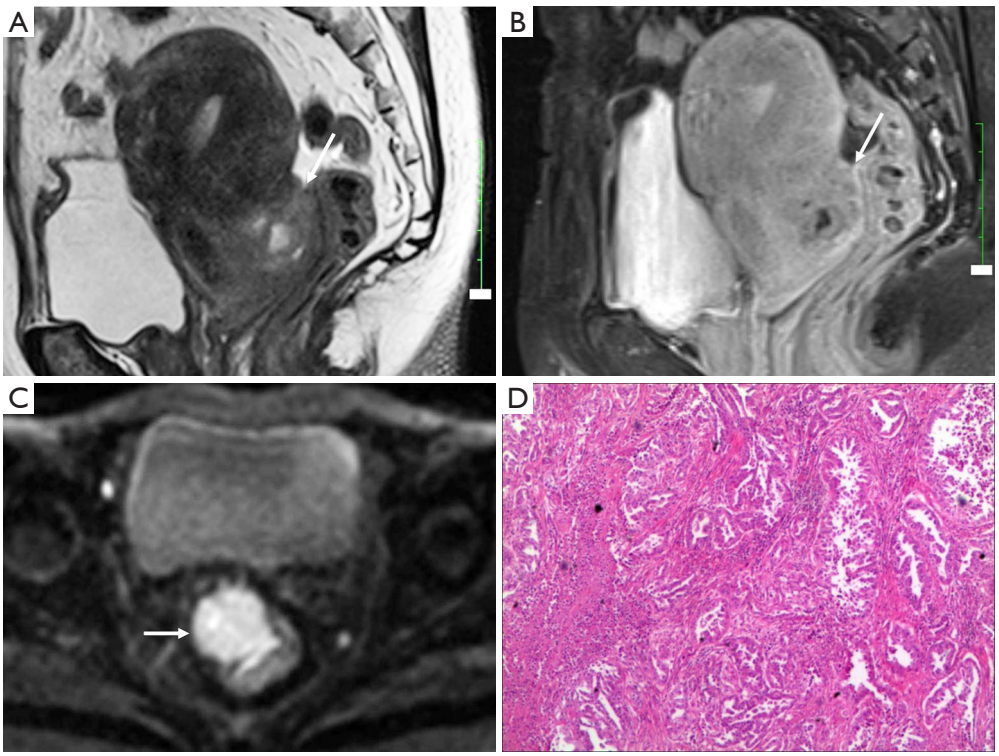

Figure 16 A 41-year-old woman with DIE and malignant transformation of the endometrial lesion in the rectovaginal septum. (A) Sagittal T2-weighted image shows a heterogeneous mass (arrow) in the rectovaginal septum; (B) sagittal contrast-enhanced fat-suppressed T1-weighted image shows moderate heterogeneous enhancement (arrow); (C) transverse diffusing-weighted image with a b value of 1,000 s/mm^2 shows obvious diffusion restriction (arrow); (D) photomicrograph (HE, ×100) shows atypical epithelial cells in glandular-tube-like, stranding and papillary arrangement.

and morphologic abnormalities and demonstrate changes consistent with laparoscopic findings. Combining signal and morphological changes, MR imaging can diagnose and evaluate extension of DIE with high accuracy, which can support surgeons in treatment decision making and patient consultation.

Acknowledgements

None.

Footnote

Conflicts of Interest: The authors have no conflicts of interest to declare.

References

1. Luciano DE, Luciano AA. Management of endometriosis-related pain: an update. Womens Health (Lond Engl) 2011;7:585-590.
2. Choudhary S, Fasih N, Papadatos D, Surabhi VR. Unusual imaging appearances of endometriosis. AJR Am J Roentgenol 2009;192:1632-44.
3. Woodward PJ, Sohaey R, Mezzetti TP Jr. Endometriosis: radiologic-pathologic correlation. Radiographics 2001;21:193-216.
4. Olive DL, Schwartz LB. Endometriosis. N Engl J Med 1993;328:1759-69.
5. Eskanazi B, Warner M. Epidemiology of endometriosis. Obstet Gynecol Clin North Am 1997;24:235-58.
6. Coutinho A Jr, Bittencourt LK, Pires CE, Junqueira F, Lima CM, Coutinho E, Domingues MA, Domingues RC, Marchiori E. MR imaging in deep pelvic endometriosis: a pictorial essay. Radiographics 2011;31:549-67.
7. Kinkel K, Chapron C, Balleyguier C, Fritel X, Dubuisson JB, Moreau JF. Magnetic resonance imaging characteristics of deep endometriosis. Hum Reprod 1999;14:1080-6.

8. Bazot M, Darai E, Hourani R, Thomassin I, Cortez A, Uzan S, Buy JN. Deep pelvic endometriosis: MR imaging for diagnosis and prediction of extension of disease. Radiology 2004;232:379-89.
9. Chen C, Hu YQ, Zhang XM. Magnetic resonance imaging features of endometrial stromal sarcoma: a case description. Quant Imaging Med Surg 2017;7:159-62.
10. Ji YF, Zhang XM, Mitchell DG, Li XH, Chen TW, Li Y, Bao ZG, Tang W, Xiao B, Huang XH, Yang L. Gastrointestinal tract involvement in acute pancreatitis: initial findings and follow-up by magnetic resonance imaging. Quant Imaging Med Surg 2017;7:641-53.
11. Glastonbury CM. The shading sign. Radiology 2002;224:199-201.
12. Togashi K, Nishimura K, Kimura I, Tsuda Y, Yamashita K, Shibata T, Nakano Y, Konishi J, Konishi I, Mori T. Endometrial cysts: diagnosis with MR imaging. Radiology 1991;180:73-8.
13. Woodward PJ, Sohaey R, Mezzetti TP Jr. Endometriosis: radiologic-pathologic correlation. Radiographics 2001;21:193-216.
14. Clement PB. Diseases of the peritoneum. In: Kurman RJ. editor. Blaustein's pathology of the female genital tract. 4th ed. New York, NY: Springer-Verlag, 1994;660-80.
15. Clement PB. Pathology of endometriosis. Pathol Annu 1990;25:245-95.
16. Heaps JM, Nieberg RK, Berek JS. Malignant neoplasms arising in endometriosis. Obstet Gynecol 1990;75:1023-8.
17. Corner GW Jr, Hu C, Hertig AT. Ovarian carcinoma arising in endometriosis. Am J Obstet Gynecol 1950;59:760-74.
18. Scully RE, Richardson GS, Barlow JF. The development of malignancy in endometriosis. Clin Obstet Gynecol 1966;9:384-411.
19. Takeuchi M, Matsuzaki K, Uehara H, Nishitani H. Malignant transformation of pelvic endometriosis: MR imaging findings and pathologic correlation. Radiographics 2006;26:407-17.
20. Busard MP, Pieters-van den Bos IC, Mijatovic V, Van Kuijk C, Bleeker MC, van Waesberghe JH. Evaluation of MR diffusion-weighted imaging in differentiating endometriosis infiltrating the bowel from colorectal carcinoma. Eur J Radiol 2012;81:1376-80.

Cite this article as: Tang X, Ling R, Gong J, Mei D, Luo Y, Li M, Xu J, Ma L. Deep infiltrating endometriosis MR imaging with surgical correlation. Quant Imaging Med Surg 2018;8(2):187-195. doi: 10.21037/qims.2018.01.10

